ELSEVIER

Microstructural development in a rapidly cooled eutectic Sn–3.5% Ag solder reinforced with copper powder

D.C. Lin [a], T.S. Srivatsan [b,*], G.-X. Wang [b], R. Kovacevic [a]

[a] *Research Center for Advanced Manufacturing, Department of Mechanical Engineering, Southern Methodist University, 1500 international PKWY, Suite #100, Richardson, TX 75081, USA*
[b] *Division of Materials Science and Engineering, Department of Mechanical Engineering, The University of Akron, Akron, OH 44325, USA*

Abstract

Experiments using eutectic Sn–3.5% Ag solder paste were conducted with the objective of examining the conjoint influence of copper particles addition and rapid cooling on microstructural development. The composite solder mixture was made by thoroughly mixing a pre-weighed amount of copper particles with a commercial Sn–3.5% Ag solder paste. The experiments were quite similar to the heating and cooling cycle of an industrial reflow soldering process. Heating of the samples was conducted in a furnace whose temperature was carefully controlled. The cooling process was conducted on a chilled aluminum block through which coolant was circulated at 0.5 °C. When the solder temperature reached 250 °C, the circulating system would turn on automatically and the sample, which is still molten, is forced to cool rapidly. Temperature records of the solder samples revealed that addition of copper particles to the eutectic Sn–3.5% Ag did not appreciably affect the heating and melting properties when compared to the unreinforced Sn–3.5% Ag counterpart. However, copper particles did change the solidification temperature of the composite solder. Detailed observations for varying amounts of copper particle addition revealed that copper particles less than 1.0 wt.% lowered the solidification temperature of the composite solder. For copper particles greater than 1.0 wt.%, the solidification temperature increased a few degrees Celsius, indicating that some of the copper particles did not completely dissolve in the Sn-dominant solder during the melting process. Results reveal that as-solidified microstructures of the eutectic Sn–3.5% Ag solder contain columnar type dendrites of the Sn-rich phase and a eutectic mixture of the Sn_3Ag and Sn-rich phase located between the dendrite columns. The addition of copper particles to the eutectic Sn–3.5% Ag solder does refine the morphology of the primary phase, which is attributed to the presence and distribution of the Cu_6Sn_5 intermetallic in the solder matrix.

1. Introduction

The discovery of the metal, lead, about a thousand years ago and its entry into the periodic table of elements attracted the attention of scientists and engineers to use it in a variety of non-critical and critical applications. For many years, lead has played a vital role in several key areas [1]. A practical example of the usage of lead, since its invention, was as an alloying addition to tin to form the lead-bearing solder (Sn–Pb). Tin-lead solder offers a combination of properties when used as a filler material for assembling electronic components [2]. However, drawbacks related to potential health hazards coupled with the toxicity of lead have gradually become more widely understood and appreciated. This has provided the impetus for viable alternatives to be chosen and used in many fields [3]. Recently, there has been increasing use of lead-free solders and related soldering processes. However, there still exists no common standard for lead-free solder alloy products [4]. The lead-free solder alloy (Sn–3.5% Ag) is considered to be a viable substitute for the traditional Sn–Pb alloys [5–10].

To improve the mechanical properties of the eutectic Sn–3.5% Ag solder and soldered joints, the composite material concept of blending reinforcement particles of either pure metal or an intermetallic compound with a solder paste has been tried.

---

* Corresponding author.
E-mail address: tsrivatsan@uakron.edu (T.S. Srivatsan).

There has been some success in obtaining a high strength solder through the composite materials approach [11–14]. For example: (a) higher shear strength and better creep properties were obtained through careful addition of nickel particles to a Sn–3.5% Ag solder [11], (b) a solder with high hardness was achieved through copper or titanium dioxide (TiO$_2$) particle addition to a 63Sn–37Pb solder [12], and (c) improved creep resistance was achieved by having copper or silver particles blend with a Sn–3.5% Ag solder [13,14]. The mechanical properties of both the solder and soldered joints can be altered by controlling the cooling rate during the soldering process. This is because the resultant microstructure is strongly dependent on the kinetics of cooling. The cooling rate at which a solder joint solidifies depends on the mutually interactive influences of (i) how fast the heat source is removed from the joint, (ii) the size of the joint, and (iii) the immediate environment surrounding the joint. Thus, the microstructure of a specific solder joint in an electronic package can be quite different depending on these parameters. It is for this reason that a comprehensive understanding of the intrinsic relationship between cooling rate, microstructural development and mechanical properties of the solder and soldered joint is essential. The intrinsic influence of cooling rate on microstructural development in lead-containing solder [15–20] and lead-free solders has been studied [21–26]. A limited number of investigations during the same time period have focused on the composite solder prepared under different cooling rates [27]. For the Sn–3.5% Ag solder, Maveety et al. [26] established a relationship between the cooling rate, microstructure and resultant mechanical properties.

In this paper, we present and discuss the effect of copper particles on kinetics of solidification of a eutectic Sn–3.5% Ag alloy through the rapid cooling process. The primary objective was to demonstrate the distribution of copper particles in a solder matrix and the formation and presence of Sn–Cu intermetallic compounds in the microstructure of the composite solder.

2. Experimental procedure

2.1. Material selection and sample preparation

A commercial no-clean Sn–3.5% Ag solder paste (average powder particle size of 45 μm) was thoroughly blended with pure copper powder (average powder particle size 1–5 μm) to form a composite solder mixture. The no-clean Sn–3.5% Ag solder was purchased from AIM Solder Corporation (Copley, Ohio, USA). Pure copper powder was purchased from Atlantic Equipment Engineers (Bergenfield, New Jersey, USA). The composite solder mixture was prepared by mechanically blending pre-weighed copper powders with the Sn–3.5% Ag solder paste. Three different copper percentages (in wt.%), namely (a) 0.5% Cu, (b) 1.0% Cu, and (c) 3.0% Cu, were chosen. The resultant mixture was stirred in a ceramic crucible using a plastic spatula. The mechanical stirring was done for 30 min to ensure a near homogeneous distribution of the reinforcing copper particles in the composite solder. Four grams of the well-mixed composite solder was placed in a stainless steel crucible having a diameter of 10 mm and mounted on a thin aluminum plate. The aluminum plate and the stainless steel crucible were placed on top of an aluminum block, which is supported inside an enclosed temperature-controlled furnace and equipped with a circulating coolant. A schematic of the test set-up is shown in Fig. 1. To have a record of the variation of temperature with time during the reflow process, a fine J-type thermocouple (diameter at 0.005 in.) was placed inside the solder paste, and the recording system used the National Instrument Lab View 5.1 program encoded with FP-TC-120 modules. The heating rate of the solder sample was around 0.8 °C/s, which is quite similar to the actual heating rate in an industrial reflow process. Once temperature of the composite solder mixture reaches 230 °C, the power to the furnace was turned off. The composite mixture was allowed to heat further because of the high temperature environment in the enclosed furnace. When temperature of the solder sample reached 250 °C, the coolant circulation was turned on so as to
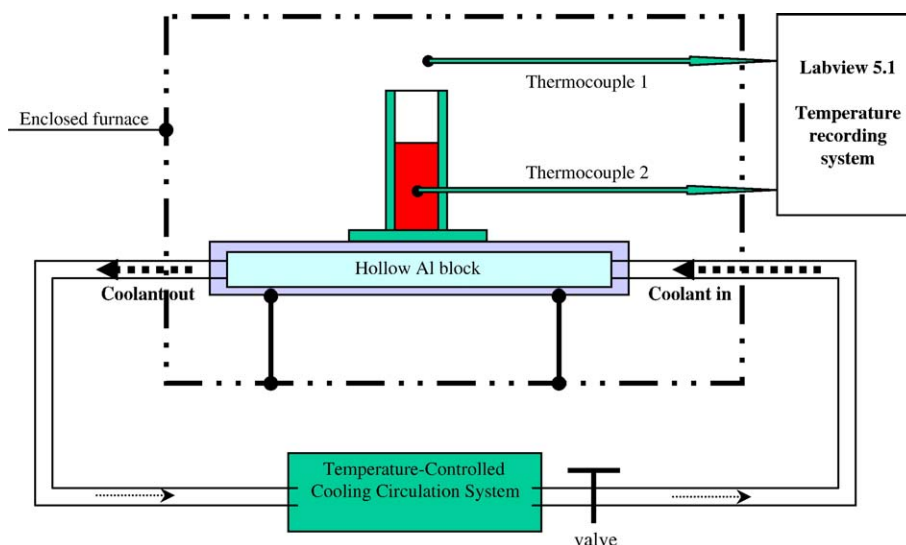

Fig. 1. A schematic of the set-up for preparing samples.

force the solder sample to cool down quickly to room temperature (27 °C). The average cooling rate in this induced rapid cooling process was calculated to be 7.5 °C/s. A profile of the temperature history during the heating and rapid cooling cycle is shown in Fig. 2.

The solder samples were thoroughly cleaned using aqueous hydrochloric acid solution to remove flux, surface oxides and other contaminants. This was followed by subjecting the composite solder sample to ultrasonic cleaning in isopropanol and drying in ambient air.

2.2. Microstructure and composition evaluation

The as-solidified samples were prepared using standard metallographic procedures for examination in an optical microscope under bright field illumination. Sample preparation involved an initial wet grind and coarse polish on progressively finer grades (320 grit, 400 grit, 600 grit, and 1000 grit) of silicon carbide impregnated emery paper using copious amounts of water as both a coolant and lubricant. The samples were then fine polished using 3-μm and 1-μm alumina powder suspended in distilled water as the coolant and lubricant. Finish polishing to a mirror-like finish was achieved using 0.3-μm and 0.05-μm diamond paste suspended in distilled water. The as-polished samples were then chemically etched using a solution mixture of nitric acid (5 ml), hydrochloric acid (2 ml) and methanol (93 ml). The polished and etched surfaces of the composite samples were observed in an optical microscope, over a range of magnification to determine: (a) size and morphology of the grains, (b) the presence, distribution and morphology of second-phase particles, and (c) size, morphology and distribution of fine microscopic pores and other artifacts in the microstructure.

Precise composition of the sample was established using energy dispersive X-ray (EDX) analysis to identify: (a) primary Sn-phase, (b) Ag_3Sn needle phase, (c) Sn–Cu intermetallic compounds, and (d) solid copper particles. Even though the overall accuracy of the EDX analysis is only moderate, the results provide a reasonable map of the variation of tin, silver, and copper components through the microstructure of the solder.

3. Results and discussion

3.1. Thermal characteristics of solder during solidification

A typical thermal history record for the solder sample during the cycle of heating, melting and rapid cooling is shown in Fig. 2. This figure provides a variation of temperature of the solder with time during the reflow process. Prior to turning the power on for making samples, the furnace with the solder sample positioned at the center is initially at room temperature (27 °C). Once the furnace is powered the solder begins to be heated. As powders of the solder progressively increase in temperature during heating, the flux immediately surrounding the solder powder provides protection against oxidation. A large portion of the flux gradually melts and flows out from the surroundings of the solder powder leaving behind solder powders having a dry layer of flux coating. As temperature of the solder in the furnace reaches its melting point, initiation of powder melting occurs. At this time, the solder sample is a blend of liquid solder and solid solder particles. For the eutectic Sn–3.5% Ag solder, the melting temperature is 221 °C. This is revealed by a small plateau in the temperature curve (Fig. 2) at which temperature the solid solder powder becomes liquid due to the absorption of latent heat. The additional copper particles did not appreciably change the melting point of the composite solder. This is because copper has a high melting point and occupies limited volume in the mixture. When the solder powder with a flux coating is completely melted, the temperature of the molten solder continues to increase. This is attributed to the driving force in the high temperature environment. The molten solder was heated to a temperature of 250 °C prior to the initiation of cooling achieved by starting the circulation system. Fig. 3(a) shows the effect of different copper percentages on the kinetics of cooling of the eutectic Sn–3.5% Ag composite solder. The four curves in this figure show the variation of undercooling and solidification temperature as a function of percentage of copper. Fig. 3(a) provides four different solidification models, which are exemplified in Fig. 3(b)–(e). Under rapid cooling conditions, the eutectic Sn–3.5% Ag alloy shown in curve 1 of Fig. 3(a) reveals non-equilibrium solidification with no obvious undercooling coupled with a plateau which is 1.8 °C lower than the melting point of eutectic Sn–3.5% Ag solder during the phase change from liquid to solid (schematic drawing shown in Fig. 3(b)).

For 0.5% copper particle addition to the Sn–3.5% Ag solder there was no evidence of undercooling, except for a short plateau with solidification occurring at 219 °C, i.e., 2 °C lower than 221 °C, the melting point prior to cooling to room temperature (Fig. 3(c)). An investigation to identify the eutectic Sn–Ag–Cu composition in annealed alloys using the differential scanning calorimetric technique reported the eutectic composition to be Sn–3.5% Ag –0.9% Cu and the eutectic temperature as 217.2 °C [28]. Addition of 0.5% copper particles results in complete
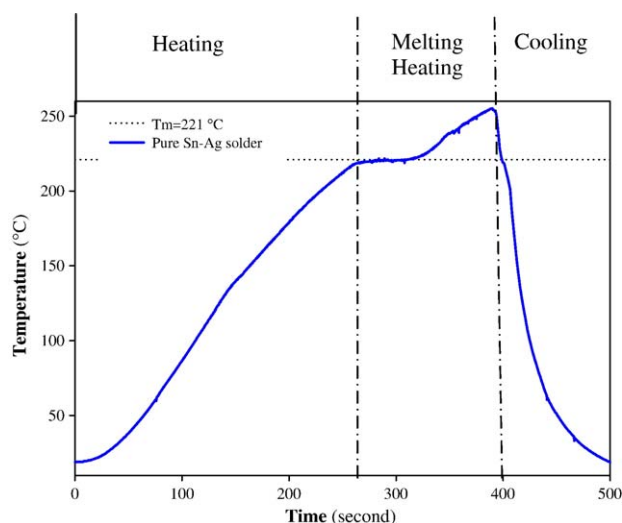

Fig. 2. Temperature recording for eutectic Sn–3.5% Ag alloy during heating and rapid cooling.
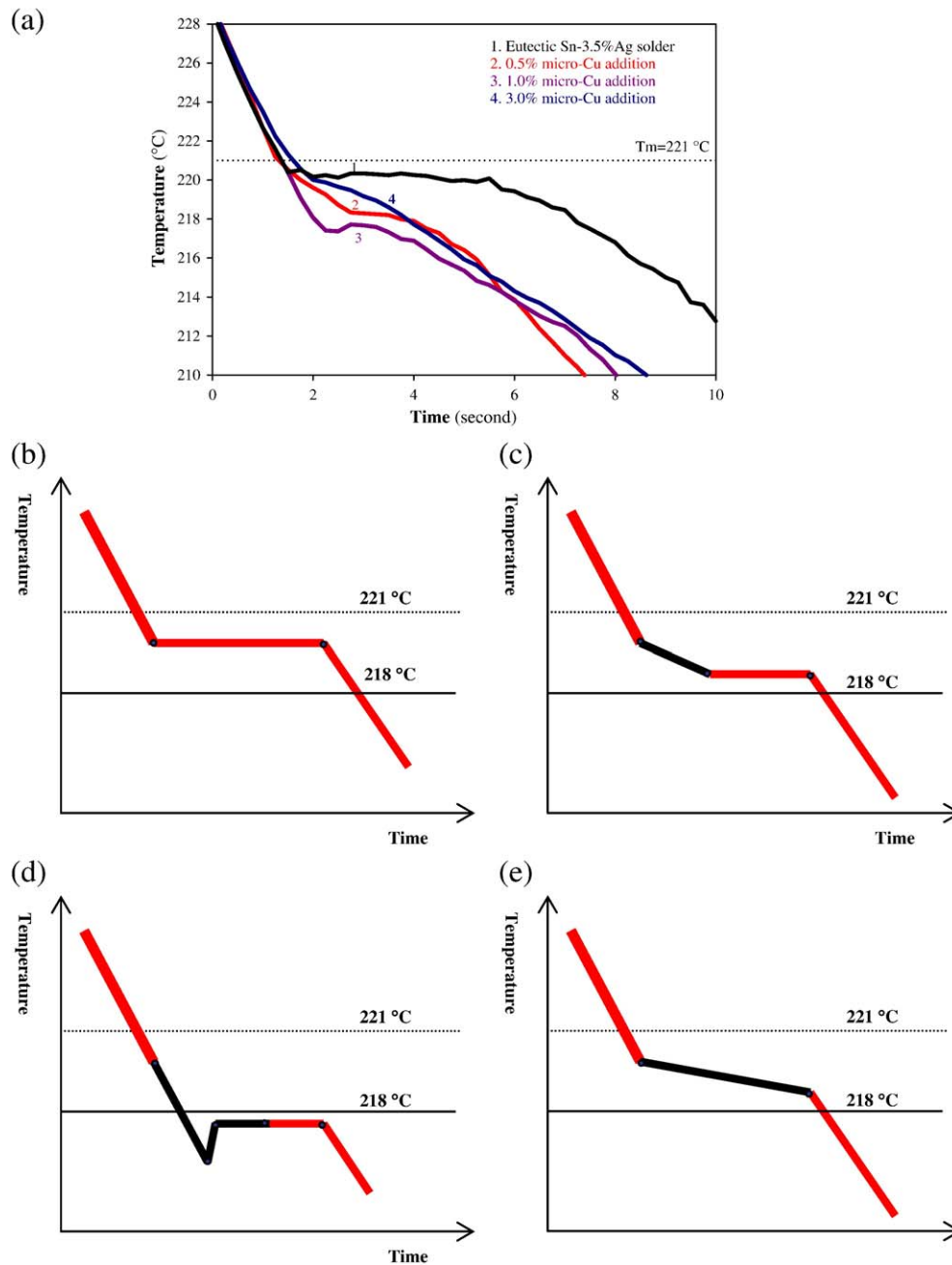
Fig. 3. Comparison of cooling curves for eutectic Sn–3.5% Ag alloy and its copper-reinforced composite alloy during rapid cooling. (a) Temperature reading to track the cooling for copper-reinforced composite solder. (b) Schematic of cooling curve for eutectic Sn–3.5% Ag. (c) Schematic of cooling curve for eutectic Sn–3.5% Ag with 0.5% copper. (d) Schematic of cooling curve for eutectic Sn–3.5% Ag with 1.0% copper. (e) Schematic of cooling curve for eutectic Sn–3.5% Ag with 3.0% copper.

dissolution in the Sn-dominant solder during the melting process.

With an increase in copper particles to 1.0%, the curve (Fig. 3(d)) reveals a 2.3 °C undercooling coupled with a short plateau and a solidification temperature of 217.5 °C. As the amount of copper particles increases to 3%, there was an absence of undercooling coupled with no distinct plateau stage (Fig. 3(e)) during solidification. This suggests that a solid copper particle and surrounding Sn–Cu intermetallic compound provide the initial nucleation site. Thus, by inducing rapid cooling, the presence of copper particles in the eutectic Sn–3.5% Ag solder

did not appreciably influence the melting process. However, the presence of copper particles does have a marginal influence on the solidification process with a concomitant influence on microstructure.

3.2. Microstructure characterization of eutectic Sn–3.5% Ag under rapid cooling

The as-solidified microstructures of the eutectic Sn–3.5% Ag after rapid cooling are shown in Fig. 4(a)–(c). The overall profile of the eutectic solders from immediately adjacent to the

bottom to top of the sample is shown in Fig. 4(a). The bottom region is marginally unstable and not considered because of direct contact with the chill block. From Fig. 4(b) and the high magnification observation (Fig. 4(c)), the microstructure reveals two distinct phases: (i) a bright tilt primary dendrite arm having a near spherical morphology second arm (EDX analysis revealed this white phase to be 97.53% Sn and 2.47% Ag as shown in Fig. 4(d), and (ii) a eutectic lamella structure comprising a mixture of the Sn-dominant phase and the small needle-like Ag_3Sn phase. The average size of the primary dendrite λ_1 (measurement shown in schematic drawing Fig. 4 (e)) is about 105 µm. This was obtained from Fig. 4(b) using the regular area counting method [29]. The secondary dendrite arm spacing λ_2 is about 15 µm (measured by averaging the distance between adjacent dendrites). The data for primary arm spacing

Table 1
The primary arm spacing λ_1 and secondary arm spacing λ_2 for rapid cooled solder

Solder	λ_1 (µm)	λ_2 (µm)
Eutectic Sn–3.5% Ag	105	15
Composite solder: Sn–3.5% Ag+0.5% Cu	150	14.5
Composite solder: Sn–3.5% Ag+1.0% Cu	60	22
Composite solder: Sn–3.5% Ag+3.0% Cu	30	10

(1) A big jump for λ_1 from 105 µm of eutectic Sn–3.5% Ag to 150 µm of 0.5% Cu-reinforced composite solder.
(2) λ_1 decreases as the copper particle added more.

λ_1 and secondary arm spacing λ_2 for eutectic Sn–3.5% Ag solder and its Cu-reinforced composite solders are listed in Table 1.
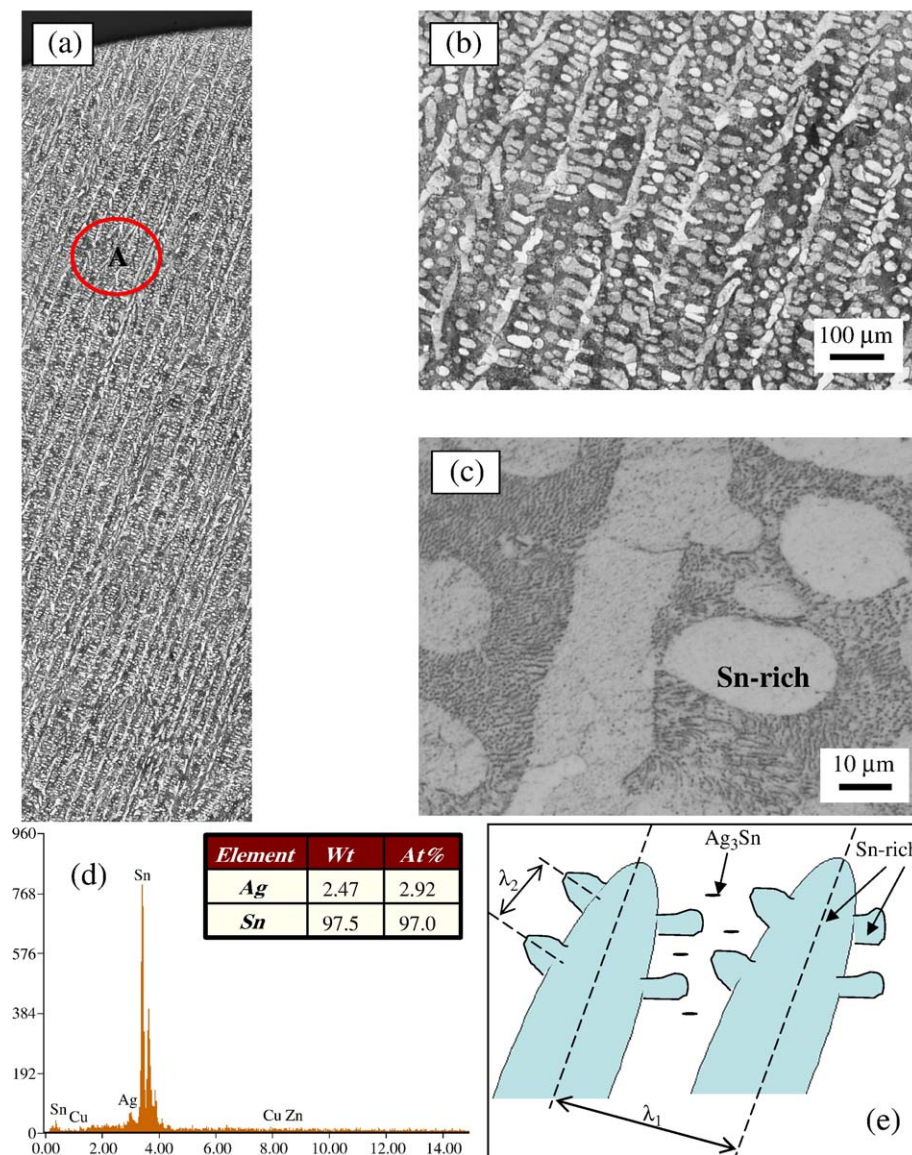

Fig. 4. Microstructure of eutectic Sn–3.5% Ag alloy after rapid solidification. (a) Lower magnification to show the overall structure from the bottom to the top. (b) Lower magnification to show the overall structure in the region A. (c) Higher magnification to show the detail structure near the bottom. (d) EDX analysis to show primary Sn-rich phase in (c). (e) Schematic illustration of eutectic lamella structure of (b) to show primary dendrite arm space λ_1 and the secondary arm space λ_2.

The observed microstructure is quite similar to reports published in the open literature on fast cooling [26]. This literature documents that an increase in the cooling rate does appreciably influence both the size and morphology of Ag₃Sn. From Fig. 4(c), the Ag₃Sn phase maintains a needle-like morphology even though it experienced rapid cooling.

3.3. Microstructure characterization of eutectic Sn–3.5% Ag with different copper particle addition under rapid cooling

The as-solidified microstructure of the eutectic Sn–3.5% Ag solder with 0.5% copper particles following rapid cooling is shown in Fig. 5(a)–(e). The overall profile of the composite solder from near the bottom to the top of the sample is shown in Fig. 5(a). From Fig. 5(b) and its higher magnification (Fig. 5

(c)), the microstructure in the mid region of the sample revealed three distinct phases.

(i) A bright dendrite phase having a near round morphology. EDX analysis indicated this white phase to be rich in tin.
(ii) The black regions other than bright Sn-rich regions are a fine mixture of the Sn-dominant phase and dispersed needle-like Ag₃Sn phase.
(iii) Small polygon-like dot phase. EDX analysis revealed this phase to be the Sn–Cu intermetallic compound Cu_6Sn_5 (Fig. 5(d)).

The primary arm spacing of the Sn-rich primary dendrite phase (measurement from Fig. 5(b)) is much larger than its
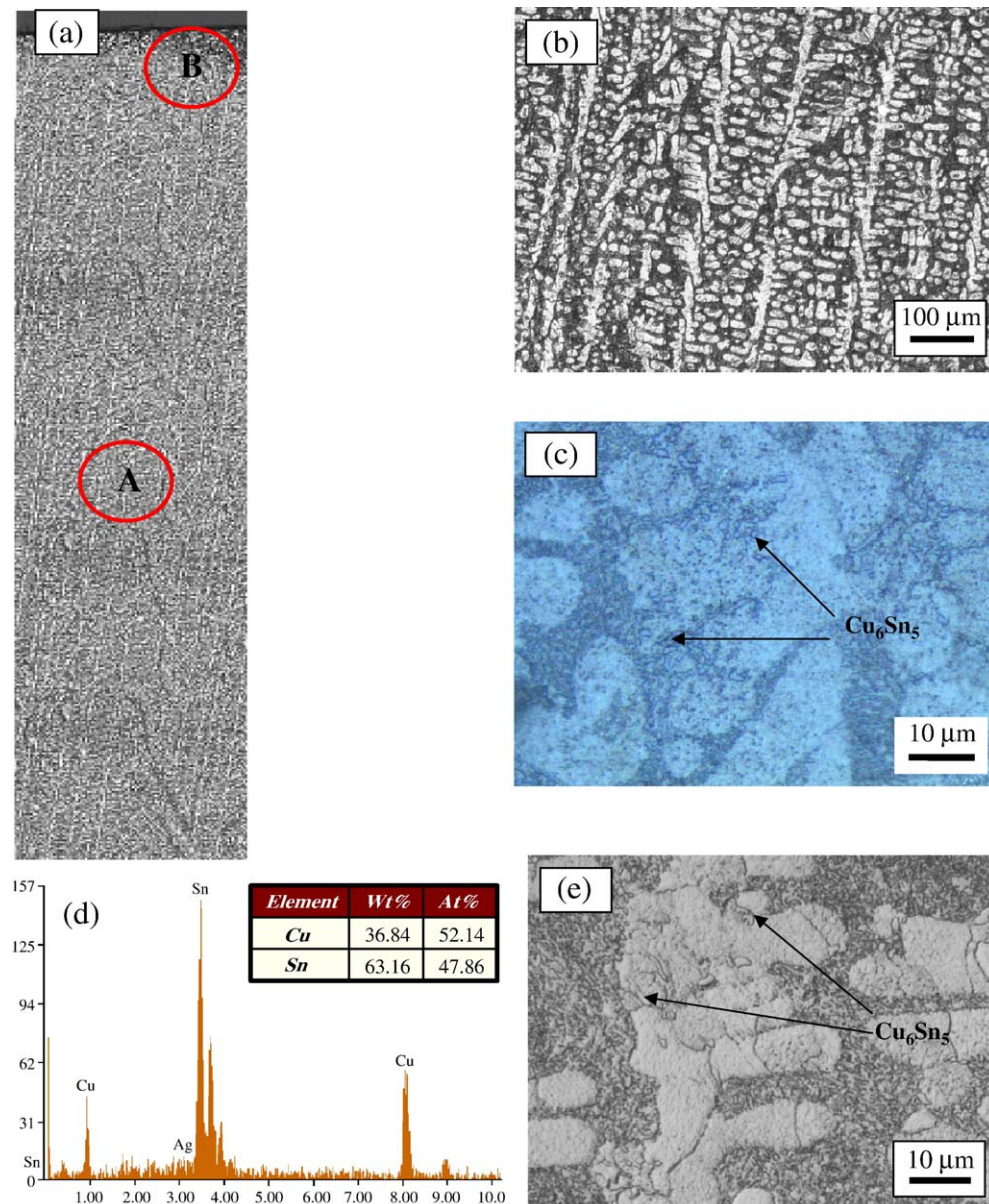

Fig. 5. Microstructure of eutectic Sn–3.5% Ag alloy with 0.5% copper after rapid cooling. (a) Lower magnification to show the overall structure from the bottom to the top. (b) Lower magnification to show the overall structure in the region A. (c) Higher magnification to show the detail structure of (b). (d) EDX analysis to show Sn–Cu intermetallic phase in (c). (e) Higher magnification to show the detail structure near the top.

counterpart for the case of the eutectic solder (Fig. 4(b)), which is about 150 μm. The secondary arm spacing for this composite solder is 14.5 μm, which is smaller than 15 μm, as shown in Table 1. Due to the formation and presence of Sn–Cu intermetallic compounds, there are more Sn-rich grains between the primary dendrites. This contributes to separation of the Cu_6Sn_5 phase. The Ag_3Sn phase in the eutectic mixture is near spherical in shape rather than needle-like as in the eutectic Sn–3.5% Ag counterpart. The microstructure near the top of the sample is shown in Fig. 5(e) and reveals the Sn–Cu intermetallic compound Cu_6Sn_5 to be larger with few of them having a needle-like morphology. In this sample, almost all of the copper particles dissolved completely in the eutectic solder

with no evidence of the presence of solid copper particles in the microstructure.

For the case of addition of more copper particles, i.e., 1.0 wt. %, to the eutectic Sn–3.5% Ag solder, the microstructure is shown in Fig. 6(a)–(e) and presents a drastically different morphology compared to the eutectic solder counterpart containing 0.5% copper addition. The Sn–Cu intermetallic compound appeared fully embedded in the Sn-rich phase (Fig. 6 (b) and (c)). The primary dendrite arm spacing is about 60 μm, while the secondary dendrite arm space is longer and about 22 μm, as shown in Table 1. The amount of near spherical shaped Sn-rich phase was drastically reduced. In the top region of the sample, evidence of un-dissolved copper (Fig. 6(f) in the EDS
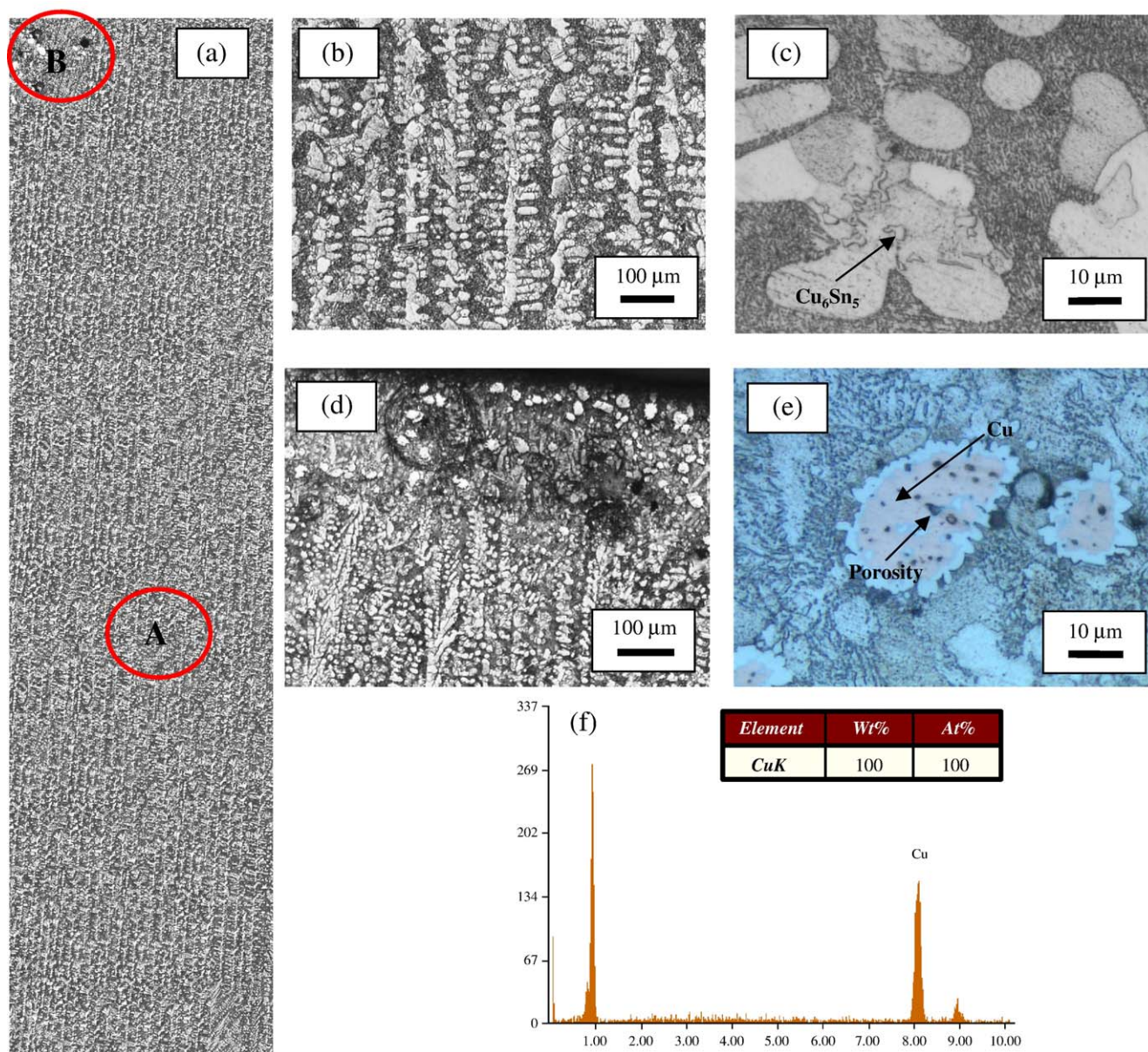

Fig. 6. Microstructure of eutectic Sn–3.5% Ag alloy with 1.0% copper particle. (a) Lower magnification to show the overall structure from the bottom to the top. (b) Lower magnification to show the overall structure in the region A. (c) Higher magnification to show the detail structure of (b). (d) Lower magnification to show the overall structure near the top region B in (a). (e) Higher magnification to show the detail structure of Sn–Cu compound. (f) EDX analysis to show the solid copper in (e).

analysis) surrounded by the Sn–Cu compound was observed (Fig. 6(d) and (e)). The sunflower morphology is quite similar to published observations [13]. This clearly indicates that even 1.0% copper exceeds its dissolvable capacity in the solder.

For 3.0% copper particle addition, the microstructural development is shown in Fig. 7(a)–(e). The microstructure reveals nearly the same morphology as the counterpart containing 1.0% copper addition. Fig. 7(b) and its higher magnification (Fig. 7(c)) reveal the Sn–Cu intermetallic compound to be well within the Sn-rich phase (Fig. 7(c)) with a polygon-like shape. The primary dendrite spacing is smaller, about 30 μm. The secondary arm spacing is shorter (about 10 μm) with a smaller number of the round Sn-rich phase

between the primary dendrites. The top region of the sample provided evidence of: (i) no-dissolved copper surrounding the Sn–Cu compound, and (ii) isolated pockets of porosity (Fig. 7d). This observation of microstructure following the rapid cooling process clearly reveals that addition of copper particles to a eutectic Sn–3.5% Ag solder paste should be kept to values of less than 1.0% when using particle reinforcement to achieve strengthening.

4. Conclusions

The following observations are made from a study on the influence of rapid cooling rate on microstructural development
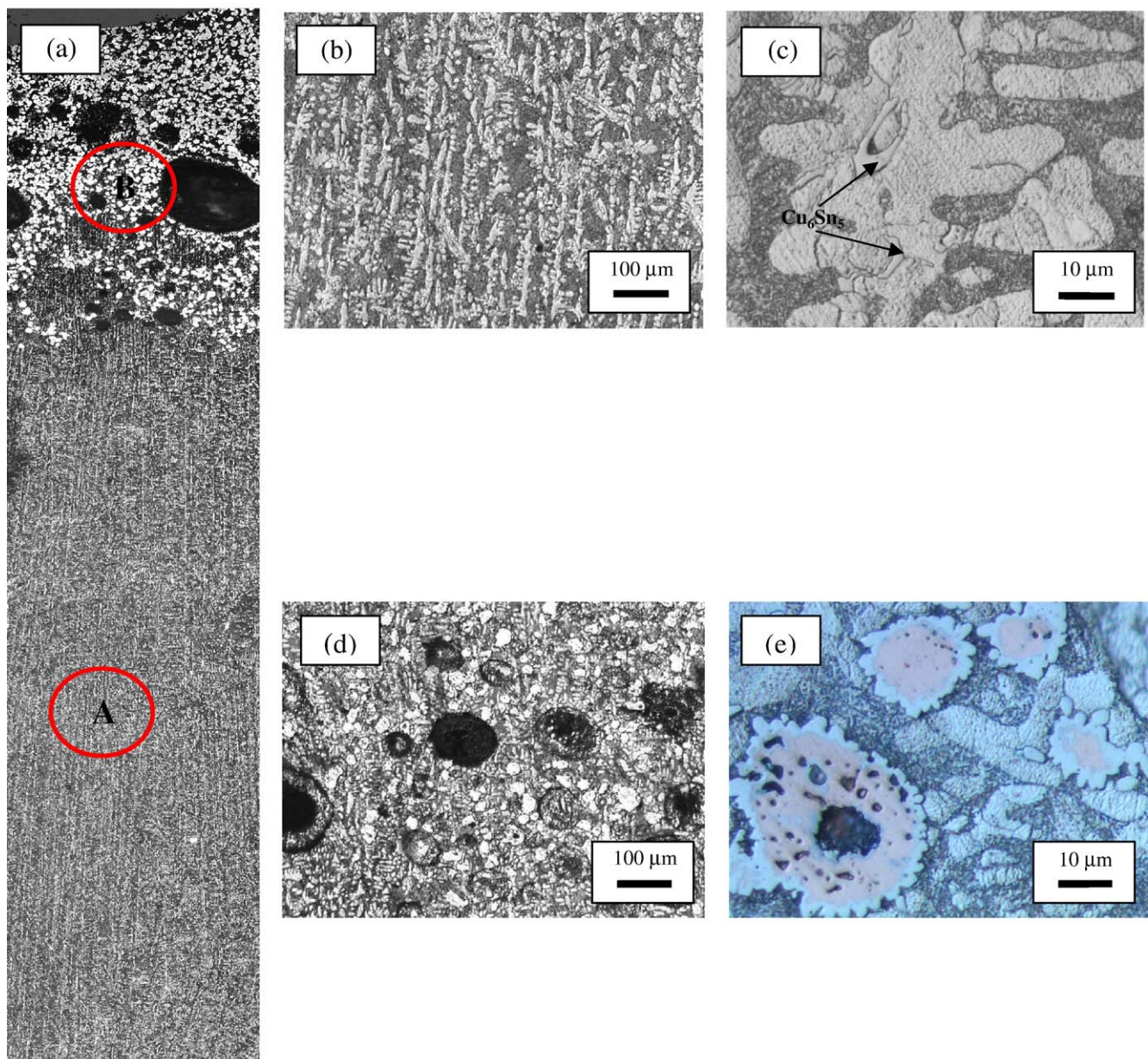

Fig. 7. Microstructure of eutectic Sn–3.5% Ag alloy with 0.5% copper particle. (a) Lower magnification to show the overall structure from the bottom to the top. (b) Lower magnification to show the overall structure in the region A. (c) Higher magnification to show the detail structure of (b). (d) Lower magnification to show the overall structure near the top region B in (a). (e) Higher magnification to show the detail structure of (d).

of a eutectic Sn–3.5% Ag solder reinforced with varying percentages of copper powders.

1) A columnar dendrite microstructure was observed because of rapid cooling of the eutectic Sn–3.5% Ag solder and the composite counterparts obtained by mixing the eutectic solder powder with copper powder.
2) 0.5 wt.% copper particle addition revealed that the copper dissolved completely in the solder from the bottom to the top.
3) In excess of 0.5 wt.% copper powders, a sunflower morphology was found in the eutectic solder with porosity located at and near the top region of the sample, and the copper particles were not completely dissolved in the eutectic solder.
4) From the standpoint of microstructural development, addition of copper powder to the eutectic Sn–3.5% Ag solder should be kept in the range of less than 1.0%.

Acknowledgments

References

[1] Martin Goosey, An overview of the current status of lead-free assembly and related issues, Circuit World 29 (4) (2003) 23–27+9.
[2] Giles Humpston, David M. Jacobson, Principles of soldering and brazing, AMS International (1993) 31–69.
[3] M. Abtew, G. Selvaduray, Lead-free solders in microelectronics, Materials Science & Engineering. R, Reports Vol. 27 (5–6) (2000) 95–141.
[4] J.H. Lau, K. Liu, Global trends in lead-free soldering part I of A II-part series on lead-free, Advanced Packaging 13 (2) (2004 (February)) 25–28.
[5] A.Z. Miric, A. Grusd, Lead-free alloys, Soldering and Surface Mount Technology 10 (1) (1998) 19–25.
[6] D. Shangguan, A. Achari, W. Green, Application of lead-free eutectic Sn–Ag solder in no-clean thick film electronic modules, IEEE Transactions on Components, Packaging, and Manufacturing Technology. Part B, Advanced Packaging 17 (4) (1994) 603–611.
[7] D. Shangguan, G. Gao, Lead-free and no-clean soldering for automotive electronics, Soldering and Surface Mount Technology 9 (2) (1997) 5–8.
[8] I. Shohji, T. Yoshida, T. Takahashi, H. Susumu, Tensile properties of Sn–Ag based lead-free solders and strain rate sensitivity, Materials Science and Engineering, A 366 (1) (2004) 50–55.
[9] H.G. Song, J.W. Morris Jr., F. Hua, The creep properties of lead-free solder joints, JOM 54 (6) (2002) 30–32.
[10] M. Kerr, N. Chawla, Creep deformation behavior of Sn–3.5Ag solder at small length scales, JOM 56 (6) (2004) 50–54.
[11] H. Rhee, F. Guo, J.G. Lee, K.C. Chen, K.N. Subramanian, Effects of intermetallic morphology at the metallic particle/solder interface on mechanical properties of Sn–Ag-based solder joints, Journal of Electronic Materials 32 (11) (2003) 1257–1264.
[12] D.C. Lin, S. Liu, T.M. Guo, G.-X. Wang, T.S. Srivatsan, M. Petraroli, An investigation of nanoparticles addition on solidification kinetics and microstructure development of tin-lead solder, Materials Science and Engineering, A 360 (1–2) (2003 (Nov 15)) 285–292.
[13] F. Guo, K.N. Subramanian, Solders strengthened with copper and silver particles, Advanced Materials and Processes 160 (12) (2002 (December)) 41–43.
[14] F. Guo, J.P. Lucas, K.N. Subramanian, Creep behavior in Cu and Ag particle-reinforced composite and eutectic Sn–3.5Ag and Sn–4.0Ag–0.5Cu non-composite solder joints, Journal of Materials Science. Materials in Electronics 12 (1) (2001 (January)) 27–35.
[15] H. Conrad, Z. Guo, Y. Fahmy, Influence of microstructure size on the plastic deformation kinetics, fatigue crack growth rate, and low-cycle fatigue of solder joints, Journal of Electronic Materials 28 (9) (1999) 1062–1070.
[16] Z. Mei, J.W. Morris, M.C. Shine, T.S.E. Summers, Effects of cooling rate on mechanical properties of near-eutectic tin-lead solder joints, Journal of Electronic Materials 20 (8) (1991) 599–608.
[17] B.S. Chiou, J.C. Cheng, Effect of cooling rate on the mechanical and electrical behaviour of a 63Sn/37Pb solder bump on a metallized Si substrate, Journal of Materials Science. Materials in Electronics 5 (4) (1994) 229–234.
[18] D.R. Frear, J.B. Posthill, J.W. Morris Jr., Microstructural details of β-Sn precipitation in a 5Sn–95Pb solder alloy, Metallurgical Transactions. A, Physical Metallurgy and Materials Science 20A (8) (1989) 1325–1333.
[19] Z. Guo, H. Conrad, Effect of microstructure size on deformation kinetics and thermo-mechanical fatigue of 63Sn37Pb solder joints, Journal of Electronic Packaging, Transactions of the ASME 118 (2) (1996 (June)) 49–54.
[20] D.P. Yao, J.K. Shang, Effect of cooling rate on interfacial fatigue-crack growth in Sn–Pb solder joints, IEEE Transactions on Components, Packaging, and Manufacturing Technology. Part B, Advanced Packaging 19 (1) (1996) 154–165.
[21] F. Ochoa, J.J. Williams, N. Chawla, Effects of cooling rate on the microstructure and tensile behavior of a Sn–3.5wt.%Ag solder, Journal of Electronic Materials 32 (12) (2003) 1414–1420.
[22] F. Ochoa, X. Deng, N. Chawla, Effects of cooling rate on creep behavior of a Sn–3.5Ag alloy, Journal of Electronic Materials 33 (12) (2004) 1596–1607.
[23] K. Noguchi, M. Ikeda, I. Shimizu, Y. Kawamura, Y. Ohno, Effect of cooling rate on microstructure and strength properties of tin–silver–copper solder ball bonding, Materials Transactions 42 (5) (2001) 761–768.
[24] K.P. Wu, N. Wade, J. Cui, K. Miyahara, Microstructural effect on the creep strength of a Sn–3.5% Ag solder alloy, Journal of Electronic Materials 32 (1) (2003 (January)) 5–8.
[25] D.C. Lin, C.Y. Kuo, T.S. Srivatsan, G.-X. Wang, Understanding solidification kinetics and microstructural development of a lead-free composite solder, American Society of Mechanical Engineers, Heat Transfer Division, (Publication) HTD 374 (3) (2003) 253–258.
[26] J.G. Maveety, O. Liu, J. Vijayen, F. Hua, E.A. Sanchez, Effect of cooling rate on microstructure and shear strength of pure Sn, Sn–0.7Cu, Sn–3.5Ag, and Sn–37Pb solders, Journal of Electronic Materials 33 (11) (2004 (November)) 1355–1362 (Nanostructured Magnetic Materials: Recent Progress in Magnetic Nanostructures).
[27] J. Sigelko, S. Choi, K.N. Subramanian, J.P. Lucas, T.R. Bieler, Effect of cooling rate on microstructure and mechanical properties of eutectic Sn–Ag solder joints with and without intentionally incorporated Cu_6Sn_5 reinforcements, Journal of Electronic Materials 28 (11) (1999) 1184–1188.
[28] M.E. Loomans, M.E. Fine, Tin–silver–copper eutectic temperature and composition, Metallurgical and Materials Transactions. A, Physical Metallurgy and Materials Science 31A (4) (2000) 1155–1162.
[29] M.S. Bhar, D.R. Poirier, J.C. Heinrich, Permeability for cross flow through columnar-dendritic alloys, Metallurgical and Materials Transactions. B, Process Metallurgy and Materials Processing Science 26 (5) (1995) 1049–1056.